The SUrvey for Pulsars and Extragalactic Radio Bursts – III. Polarization properties of FRBs 160102 and 151230

M. Caleb,[1,2,3,4]★ E. F. Keane,[3,4,5] W. van Straten,[6] M. Kramer,[1,7] J. P. Macquart,[8]
M. Bailes,[3,4] E. D. Barr,[3,4,7] N. D. R. Bhat,[4,8] S. Bhandari,[3,4,9] M. Burgay,[10] W. Farah,[3]
A. Jameson,[3,4] F. Jankowski,[1,3,4] S. Johnston,[9] E. Petroff,[3,4,9,11] A. Possenti,[10]
B. W. Stappers,[1] C. Tiburzi[12] and V. Venkatraman Krishnan[3,4]

[1]*Jodrell Bank Centre for Astrophysics, School of Physics and Astronomy, The University of Manchester, Manchester M13 9PL, UK*
[2]*Research School of Astronomy and Astrophysics, Australian National University, ACT 2611, Australia*
[3]*Centre for Astrophysics and Supercomputing, Swinburne University of Technology, PO Box 218, Hawthorn, VIC 3122, Australia*
[4]*ARC Centre of Excellence for All-sky Astrophysics (CAASTRO), Sydney, NSW, Australia*
[5]*SKA Organization, Jodrell Bank Observatory, Cheshire SK11 9DL, UK*
[6]*Institute for Radio Astronomy and Space Research, Auckland University of Technology, Private Bag 92006, Auckland 1142, New Zealand*
[7]*Max-Planck-Institut für Radioastronomie, Auf dem Hügel 69, D-53121 Bonn, Germany*
[8]*International Centre for Radio Astronomy Research, Curtin University, Bentley, WA 6102, Australia*
[9]*CSIRO Astronomy and Space Science, Australia Telescope National Facility, PO Box 76, Epping, NSW 1710, Australia*
[10]*INAF – Osservatorio Astronomico di Cagliari, Via della Scienza 5, I-09047 Selargius (CA), Italy*
[11]*ASTRON, The Netherlands Institute for Radio Astronomy, Postbus 2, NL-7990 AA Dwingeloo, the Netherlands*
[12]*Fakultät fur Physik, Universität Bielefeld, Postfach 100131, D-33501 Bielefeld, Germany*

ABSTRACT

We report on the polarization properties of two fast radio bursts (FRBs): 151230 and 160102 discovered in the SUrvey for Pulsars and Extragalactic Radio Bursts (SUPERB) at the Parkes Radio Telescope. FRB 151230 is observed to be 6 ± 11 per cent circularly polarized and 35 ± 13 per cent linearly polarized with a rotation measure (RM) consistent with zero. Conversely, FRB 160102 is observed to have a circular polarization fraction of 30 ± 11 per cent, linear polarization fraction of 84 ± 15 per cent for RM $= -221(6)$ rad m^{-2}, and the highest measured dispersion measure (2596.1 ± 0.3 pc cm^{-3}) for an FRB to date. We examine possible progenitor models for FRB 160102 in extragalactic, non-cosmological and cosmological scenarios. After accounting for the Galactic foreground contribution, we estimate the intrinsic RM to be $-256(9)$ rad m^{-2} in the low-redshift case and $\sim -2.4 \times 10^2$ rad m^{-2} in the high-redshift case. We assess the relative likeliness of these scenarios and how each can be tested. We also place constraints on the scattering measure and study the impact of scattering on the signal's polarization position angle.

Key words: magnetic fields – polarization – methods: data analysis – surveys – intergalactic medium.

1 INTRODUCTION

Radio astronomy is exploring – with progressively increasing effectiveness – an intriguing phase space of the dynamic Universe on time-scales of milliseconds. The recent development of sensitive, high time-resolution instruments over the last decade has enabled the discovery of millisecond duration fast radio bursts (FRBs; Lorimer et al. 2007). FRBs are characterized by dispersion measures (DMs) that are too much large to be accounted for by the Galaxy (Thornton et al. 2013; Champion et al. 2016). All FRBs exhibit a power-law-dependent time delay consistent with ν^{-2}, which is characteristic of propagation through a cold ionized diffuse medium.

FRB theories can be broadly classified into two categories: cataclysmic and non-cataclysmic production scenarios. Cataclysmic progenitors are predicted as relatively rare explosive collisions between pairs of white dwarfs, or of old neutron stars (e.g. Kashiyama, Ioka & Mesaros 2013; Totani 2013; Fuller & Ott 2015), or supermassive neutron stars collapsing into black holes (Falcke & Rezzolla 2014). Examples of non-cataclysmic progenitors are more common – periodic flares or outbursts from rotating neutron-stars-like

★ E-mail: manishacaleb@gmail.com

pulsars and magnetars (e.g. Pen & Connor 2015; Connor, Sievers & Pen 2016; Cordes & Wasserman 2016). The explosion-based models suggest that FRBs are energetic, singular events, while the outbursts-based models suggest that FRBs are less energetic and repeating. The examples here by no means exhaust the various models proposed in the literature. However, despite being broadly classified as FRBs, each pulse appears to be unique in its own way (in terms of temporal pulse broadening, scintillation, frequency structure, and polarization properties) hindering a consensus for their origin.

Several studies have reported the potential of using FRBs as a cosmological probe to solve the 'missing baryons' problem (McQuinn 2014; Keane et al. 2016), acquire an independent measure of the dark energy equation of state (Zhou et al. 2014), and study the intergalactic magnetic field (Zheng et al. 2014; Ravi et al. 2016). Since FRBs are highly energetic pulses of coherent emission of very short duration, their polarization properties could prove vital to understanding the unknown generation and evolution of magnetic fields in the Universe. Faraday rotation is a birefringence effect in which the angle of the linearly polarized light of a radio wave is rotated under the influence of a magnetized plasma. The amount of rotation undergone is quantified by the rotation measure (RM) and can be approximated to be

$$RM = 0.810 \int_0^D n_e B_{||} \, dl \, \text{rad m}^{-2}, \tag{1}$$

where n_e is the electron density along the line of sight (LOS) in particles cm^{-3}, $B_{||}$ is the vector magnetic field parallel to the LOS in microgauss (G), and dl is the elemental vector towards the observer along the LOS. The sign of the RM quantity is such that a field oriented towards the observer is positive and away from the observer is negative. An important advantage of Faraday rotation is that it is observable in any plasma irrespective of whether or not those atoms/molecules have magnetically susceptible energy levels. This indicates that we can ignore interstellar extinction and thus probe magnetic fields out to cosmological distances. The magnitudes of pulsar RMs range from very small values or order less than 1 rad m^{-2} (Han et al. 2006; Noutsos et al. 2008; Schnitzeler 2010) to $(-6.696\pm0.005) \times 10^4$ rad m^{-2} for the magnetar J1745−2900, near Sagittarius A∗ at the centre of our Galaxy (Eatough et al. 2013; Desvignes et al. 2018). There can be up to ∼10 rad m^{-2} (also depending on the time of day) of contribution to the RM from the Earth's ionosphere (Kronberg 2016). Recently, the repeating FRB 121102 (also referred to as 'the repeater' in this paper) discovered at the Arecibo telescope in Puerto Rico was found to be 100 per cent linearly polarized with an average RM $= (+1.027\pm0.001) \times 10^5$ rad m^{-2} (Michilli et al. 2018), which is the largest measured RM of an extragalactic source to date. RMs of this magnitude have only been observed near the vicinities of black holes with masses $>10^4$ M$_\odot$, an example of which is the supermassive black hole Sagittarius A∗ at the centre of our Galaxy, with RM $= (-4.3\pm0.1) \times 10^5$ rad m^{-2} (Bower et al. 2003; Marrone et al. 2007).

Of the 28 published FRBs[1] (Petroff et al. 2016) only six have polarization information (Masui et al. 2015; Petroff et al. 2015, 2017; Keane et al. 2016; Ravi et al. 2016; Michilli et al. 2018) due to the fact that only Stokes I is preserved in typical searches. It should be noted that the FRBs discovered at the UTMOST telescope also have only Stokes I recorded due to the antennas being only right

circularly polarized. The total intensity of the signal is defined as $I \geqslant \sqrt{Q^2 + U^2 + V^2}$, where Q and U are the linearly polarized components of I, and V is the circularly polarized component of I. The total linear polarization is defined as $L = \sqrt{Q^2 + U^2}$.

An important feature of FRBs, if they are indeed cosmological, is that the observed total rotation measure (RM$_{tot}$) would then be a combination of different contributions:

$$RM_{tot} = RM_{iono} + RM_{Gal} + RM_{IGM}$$
$$+ RM_{host} + RM_{source}, \tag{2}$$

where RM$_{iono}$ is the RM due to the Earth's ionosphere (Sotomayor-Beltran et al. 2013), RM$_{Gal}$ is the Galactic component assumed to typically vary with Galactic latitude and longitude and includes the local universe RM contributions, RM$_{IGM}$ is the contribution from the intergalactic medium (IGM) in the form of galaxies or filaments of cosmological large-scale structures along the LOS, RM$_{host}$ is the RM due to anomalous regions in a host galaxy, and RM$_{source}$ is the 'intrinsic' component from magnetized plasma associated with the progenitor source and its immediate environment. In the case of a source at cosmological distances, the RM along the LOS after accounting for the contributions from RM$_{Gal}$ and RM$_{iono}$ will be reduced by a factor of $(1 +z)^2$ as

$$RM(z) = 0.810 \int_0^z \frac{n_e(z) B_{||}(z)}{(1 + z)^2} \frac{dl}{dz} \, dz \tag{3}$$

due to the redshifting of the observed frequencies. Based on the RM and DM, the average magnetic field along the LOS can be estimated as

$$\langle B_{||} \rangle \simeq 1.232 \left(\frac{RM}{\text{rad m}^{-2}} \right) \left(\frac{DM}{\text{pc cm}^{-3}} \right)^{-1} \text{G}. \tag{4}$$

It should be noted that the above equation does not include the redshift correction, which can be accounted for by replacing DM by DM/$(1 +z)$ (Akahori, Ryu & Gaensler 2016). The average magnetic field along the LOS can be affected by (1) the presence of electron density inhomogeneities such as a hot nebula or H$_{II}$ region (Bannister & Madsen 2014) that will dominate and cause the magnetic field to be overestimated; and (2) field reversals occurring along the sightline similar to the ones we see between the spiral arms of the Milky Way (Han et al. 2006). In both cases the individual components in equation (2) cannot be measured independently and therefore the large-scale magnetic field along a given LOS cannot be accurately estimated.

For FRB 140514 observed at Parkes, a significant circularly polarized ($V = 21 \pm 7$ per cent) component was observed and no RM could be measured (Petroff et al. 2015). For FRB 110523 observed at the Green Bank Telescope (GBT), the signal was significantly linearly polarized ($L = 44 \pm 3$ per cent, $V = 23 \pm 30$ per cent) with a large RM of $-186.1.1 \pm 1.4$ rad m^{-2} (Masui et al. 2015). FRB 150807 discovered at Parkes was found to be highly linearly polarized with a fraction of $L = 80 \pm 1$ per cent and an RM of 12.0 ± 7 rad m^{-2} (Ravi et al. 2016). However, the measured RM of FRB 150807 is probably dominated by the same contributions seen towards the pulsar J2241−5236 (+13.3 rad m^{-2}) located along a nearby sightline. Ravi et al. (2016) estimate the RMs due to magnetic fields in the region of detection (Galactic halo at high Galactic latitude) to be much smaller than that of the pulsar and therefore adopt the pulsar RM as the Galactic contribution for the given LOS. FRB 150215 (Petroff et al. 2017) and FRB 150418 (Keane et al. 2016) were also found to be linearly polarized $L= 43 \pm 5$ and 8.5 ± 1.5 per cent, respectively, but yielded RMs consistent with zero. More recently, as anticipated above, the repeating FRB 121102

---

[1] All published FRBs and their measured properties are available on the FRB Catalogue http://www.frbcat.org

was found to be 100 per cent linearly polarized with a large RM of $(+1.027 \pm 0.001) \times 10^5$ rad m^{-2}. No obvious trend has emerged from the small sample of FRB RMs (see Table 1). Bhandari et al. (2018) report the detections of four new FRBs discovered in the SUrvey for Pulsars and Extragalactic Radio Bursts (SUPERB; Keane et al. 2018). Two of these were detected in real-time with full polarization information. Here we present the polarization analyses of these FRBs 151230 and 160102.

2 OBSERVATIONS AND ANALYSES

2.1 Observing set-up

SUPERB uses the 21-cm multibeam receiver (Staveley-Smith et al. 1996) at the Parkes Radio Telescope along with the Berkeley Parkes Swinburne Recorder (BPSR) backend instrument to obtain data. BPSR records 8-bit full polarization data from two orthogonal linear feeds per beam for each of the 13 beams of the multibeam receiver over 400 MHz bandwidth from 1182 to 1582 MHz with 1024 channels at 64-s time resolution. This 8-bit data is sent to a 120-s ring buffer and is processed in real-time using the HEIMDALL single pulse search software. If HEIMDALL identifies a candidate matching the criteria in equation (1) of Keane et al. (2018), it saves the 8-bit data in the buffer within the time window $t_0 - \Delta t \leq t \leq t_0 + 2\Delta t$, where t_0 is the time at which the event occurred at the highest frequency of the observing band, t is the time elapsed since the start of the observation, and Δt is the dispersive delay across the whole band for the total observed DM.

FRBs 151230 and 160102 reported in Bhandari et al. (2018) were detected in beams 03 (inner hexagon) and 13 (outer hexagon) of the multibeam receiver at DMs of 960.4±0.5 and 2596.1±0.3pc cm^{-3}, respectively. Data from all 13 beams of the receiver were analysed in detail and no detection was visible in any of the neighbouring beams above a signal-to-noise ratio (S/N) threshold of 6. Hence we classify them as single-beam detections.

2.2 Polarization calibration

At Parkes, each of the 13 beams of the multibeam receiver is equipped with two orthogonal linear feeds to measure the electric field vectors E_x and E_y of the X and Y components of the incoming radiation. A calibration probe is placed at a 45° angle to the signal probes to enable the injection of a linearly polarized broad-band pulsed calibration signal. We used standard calibration techniques from the PSRCHIVE[2] package. We adopt the ideal feed assumption (IFA) according to which the receptors are perfectly orthogonally polarized, and the reference source is 100 per cent linearly polarized and illuminates both receptors equally and in phase. We do not adopt the Measurement Equation Template Matching (METM) model (van Straten 2013) as the uncertainty of the FRB position in the beam and the potential variation of polarimetric response with position in the beam make the precision of METM unnecessary. In keeping with the IAU/IEEE convention, for the Parkes 21-cm Multibeam Receiver we set the symmetry angle to $-\pi/2$ (van Straten et al. 2010). A calibration of the gain and phase of the receiver system was done by recording a pulsed calibration signal for 2 min after the detections. Calibration data were recorded 45.4 and 1.2 h after the detections of FRBs 151230 and 160102, respectively. We note

that no changes were made to the observing set-up between the discovery and calibration observations of FRB 151230.

Ravi et al. (2016), after extensive testing, conclude that the receptors in the central beam 01 of the multibeam receiver exhibit cross-coupling at the 10 per cent level. Assuming the response of the other beams to be similar, Ravi et al. (2016) expect the fractional error in measurement of their polarization for the FRB reported in their paper to be <10 per cent. The positional uncertainty of the FRB in the beam of detection might affect the degree of polarization. The attenuation of the polarization due to this uncertainty has been empirically modelled and studied in Ravi et al. (2016). Tests to measure the RM and study the polarization profile of PSR J1644−4559, which is a good calibrator due to its stable flux density, at various on- and off-axis beam positions for all the 13 beams were found to be consistent with the values and profiles in published literature (Johnston 2004; Han et al. 2006). Thus even in the case of the most extreme offset from the true position of FRBs, we do not expect the polarization measured to be significantly different from the intrinsic properties except in the unlikely event that it is present in a sidelobe of the beams in the outer hexagon of the Parkes multibeam, in which case further investigation is required.

3 RESULTS

We present the polarization profiles of FRBs 151230 and 160102 in Fig. 1. To determine the RM, the data were processed using both a brute-force search method with RMFIT[3] described in Hotan, Bailes & Ord (2005) and the RM synthesis method as described in Macquart et al. (2012).

3.1 Brute-force search with RMFIT

In the brute-force search method with RMFIT, we determine the RM by integrating in frequency for a range of trial RMs between $\pm 1.2 \times 10^5$ rad m^{-2} in steps of 1 rad m^{-2} and search for a peak in the total linearly polarized intensity $L = \sqrt{Q^2 + U^2}$ (see Fig. 2). The searched RM range was determined by accounting for the maximum RM that we can measure within a single channel after which the signal would be completely depolarized. The Stokes parameter profiles are produced for the upper and lower band profiles after correcting for the RM value corresponding to the peak in linearly polarized intensity in the previous step. The best estimate of the RM is then obtained by taking the weighted mean position angle difference between the two bands with the weight inversely proportional to the square of the error in position angle difference for each pulse phase bin.

The linear polarization never exceeded the S/N threshold of 3σ in the case of FRB 151230 and no RM value could therefore be recovered. This FRB is seen to have average linear and circular polarization fractions of $L = 35 \pm 13$ per cent, $V = 6 \pm 11$ per cent at RM = 0. We however recover an RM of -220.6 ± 6.4 rad m^{-2} for FRB 160102 as shown in Fig. 2. This FRB is seen to have average linear and circular polarization fractions of $L = 84 \pm 15$ per cent, $V = 30 \pm 11$ per cent at the measured RM. The measured RM implies a LOS magnetic field strength of $B \gtrsim 0.1$ G, which is a lower limit due to possible LOS magnetic field reversals caused by intervening components-like filaments or galaxies.

Table 1. Summary of the polarization properties measured in the FRB sample available so far. The second and third columns list the observed fractional linear and circular polarization, respectively.

FRB name	L (per cent)	V (per cent)	Total RM (rad m^{-2})	Galactic RM (rad m^{-2})	Reference
110523	44 ± 3	23 ± 30	-186.1 ± 1.4	18 ± 13	Masui et al. (2015)
121102	100	–	$+1.026 \pm 0.001 \times 10^5$	-25 ± 80	Michilli et al. (2018)
140514	<10	21 ± 7	–	–	Petroff et al. (2015)
150215	43 ± 5	3 ± 1	$-9 < RM < 12$	–	Petroff et al. (2017)
150418	8.5 ± 1.5	–	36 ± 52	–	Keane et al. (2016)
150807	80 ± 1	–	12.0 ± 7	13.3	Ravi et al. (2016)
151230	35 ± 13	6 ± 11	–	–	This work
160102	84 ± 15	30 ± 11	-220.6 ± 6.4	24.6	This work
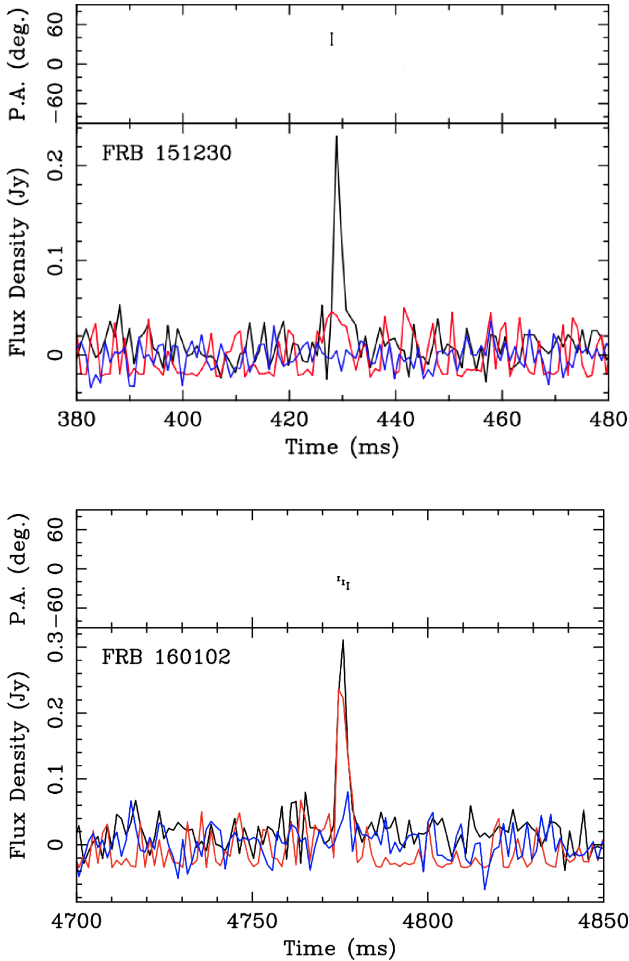
Figure 1. Polarization profiles of FRBs 151230 (top) and 160102 (bottom) after RM correction. Top panel: polarization position angles of the electric field vectors across the on-pulse phase bins. Bottom panel: the total intensity (black), total linear polarization (red), and total circular polarization (blue) are shown as a function of time. FRB 151230 is seen to have linear and circular fractions of $L = 35 \pm 13$ per cent and $V = 6 \pm 11$ per cent assuming RM $= 0$ rad m^{-2} (see text for details), and FRB 160102 is seen to have linear and circular fractions of $L = 84 \pm 15$ per cent and $V = 30 \pm 11$ per cent after correcting for RM $= -220.6$ rad m^{-2}. The data are not flux calibrated and the flux densities are in arbitrary units.

3.2 Rotation measure synthesis

The technique of RM synthesis (Brentjens & de Bruyn 2005) was applied to the channelized Q and U measurements of FRBs 151230 and 160102. For each trial RM value, this algorithm calculates
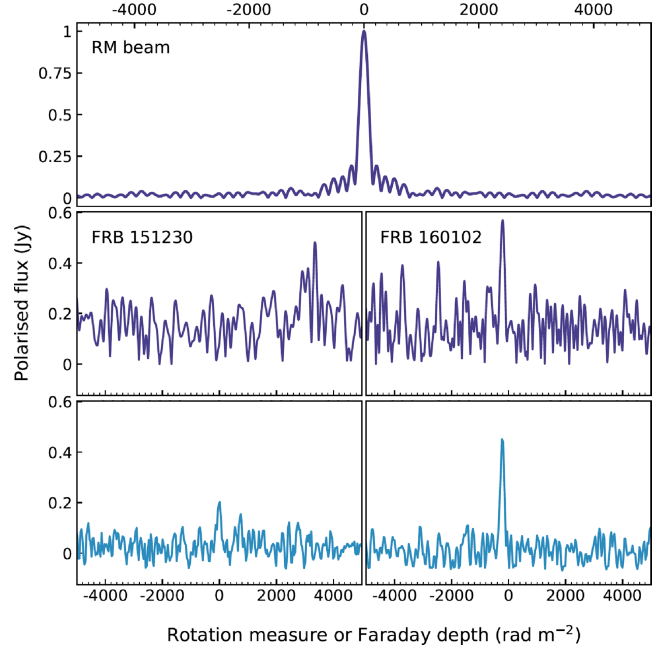

Figure 2. The RM spectra (not deconvolved) of FRB 151230 (middle, left) and FRB 160102 (middle, right) from the RM synthesis method show the amplitude of the polarized signal obtained by winding up the channelized (Q, U) vectors for a range of trial RM values as described in Section 3.2. The top panel shows the RM 'beam', which is the instrumental response to a polarized signal of unit amplitude at RM $= 0$ rad m^{-2}. Brute-force searches for RM using RMFIT for FRB 151230 (bottom, left) and FRB 160102 (bottom, right) were performed by looking for peaks in the linearly polarized flux density. A peak in the linearly polarized intensity is seen at RM $= -220.6 \pm 6.4$ rad m^{-2} for FRB 160102 and no significant RM was recovered for FRB 151230. The polarization amplitude is in arbitrary units.

the amplitude of the summation of the channelized vectors (Q, U) after derotation by the appropriate angle for that frequency and RM value. At trial RM values that do not correspond to the correct RM value, the (Q, U) vectors add incoherently, and the resultant polarization amplitude is consistent with the amplitude of the noise in the RM spectrum. However, when the trial RM corresponds to the true RM of the signal, the derotated (Q, U) vectors sum coherently, and equal the amplitude of the polarized signal. We used the implementation of this algorithm described in Macquart et al. (2012) to search for Faraday rotation of the polarized signals on grids with 1 rad m^{-2} resolution over Faraday depths spanning the range $\pm 1.2 \times 10^5$ rad m^{-2} to be consistent with Section 3.1. RM synthesis includes the additional step of using a variation of CLEAN to deconvolve the RM transfer function from the approximation to

the Faraday dispersion function. This additional step differentiates RM synthesis from the brute-force search implemented by RMFIT.

Table 2 lists the Faraday depths of the highest S/N polarized features detected and the resulting reduced χ^2 value when a signal with the amplitude and RM obtained is applied to the data. In fact, it is important to test any signal against the hypothesis that it is a spurious noise spike. One obvious test of any putative signal is to examine to what extent a signal of the derived amplitude and Faraday depth, when subtracted from the raw polarization data, results in a measurable decrease in the variance of the remaining signal. Ideally, the residual of a signal of the correct amplitude and Faraday depth subtracted from the data should be consistent with thermal noise. Thus, subtraction of the correct polarization model from the raw data should have a reduced χ^2 value close to unity. A signal whose subtraction from the raw data results in little or no reduction in the reduced χ^2 is unlikely to be real. Fig. 2 shows the amplitude of the polarized signal as a function of Faraday depth for each of these two bursts before deconvolution.

For FRB 160102, the S/N of the polarized signal associated with a Faraday depth of -210 ± 13 rad m^{-2} reaches 6, and subtraction of this signal from the data yields a residual signal that is consistent with noise (with a reduced χ^2 value of 1.4). This value of RM for FRB 160102 is consistent with the value obtained with RMFIT in the previous section. However, we are less confident of the peak in signal at RM = 3355 ± 15 rad m^{-2} detected in FRB 151230 (see Table 2). Although its S/N of 6 suggests that the signal is real at a >98 per cent confidence level,[4] various benchmark tests of RM synthesis codes against objects of known RMs show that events at S/N ~ 6–7 are close to the threshold of believability for this algorithm (Macquart et al. 2012; Schnitzeler & Lee 2015). This is because the distribution of polarization amplitudes returned by the RM search is positive, definite, and non-Gaussian, with a tail that extends to high S/N values; this is important in the present case, in which the search spans a range of 2.4×10^5 rad m^{-2} in Faraday depth, with an RM beamwidth of approximately 120 rad m^{-2}. Moreover, the reduced χ^2 after this polarized signal is applied to the data is much larger at 2.4 thereby making unlikely the possibility of it being real.

Finally, in addition to the peak at 3355 rad m^{-2} in the FRB 151230 spectrum, peaks at $\sim$2500 and $\sim$4000 rad m^{-2} in the FRB 160102 spectrum are also not robust to changes in the parameters of the search grid, indicating that they are unlikely to be genuine. The RM from FRB 160102 however survives all of these tests giving us confidence that is a genuine astrophysical RM signature.

3.3 Galactic foreground and extragalactic contribution to rotation measure

The RM contribution to FRB 160102 from the Galactic foreground was estimated in three different ways: using nearby extragalactic polarized sources, RMs of pulsars in our Galaxy, and from available RM maps (see Fig. 3). In the first method, we identified the RM of the closest known NRAO VLA Sky Survey (NVSS; Taylor, Stil & Sunstrum 2009) source. NVSS J224509−301243 is $\sim 2°$ away from the position of the FRB, has an RM of $+28.7 \pm 6.3$ rad m^{-2}. In the second method, the closest known pulsar J2155−3118 is $\sim 10°$ away and has an RM of $+33.8 \pm 14.4$ rad m^{-2} (Han et al. 2018).

[4]See table 1 and associated text in Macquart et al. (2012) for a discussion of confidence as a function of S/N.

In the third method, the contribution from the smoothed Galactic foreground (Oppermann et al. 2015) maps was estimated to be $+22 \pm 6$ rad m^{-2}. The foreground contributions from all three methods are seen to be consistent with an average of $+28 \pm 6$ rad m^{-2}. The IGM can contribute $\lesssim \pm 7$ rad m^{-2} along a typical LOS out to the maximum estimated redshift of the FRB, $z \leq 2.1$ (Oppermann et al. 2015). Based on these values and the RM obtained from RMFIT we can estimate the (RM$_{source}$ + RM$_{host}$) contribution from equation (2), as -256 ± 9 rad m^{-2} not taking into account the redshifting of frequency.

4 DISCUSSION

FRB 160102 is found to have an RM well in excess of what can be accounted for by both our Galaxy and the IGM. This is indicative of magnetization in the immediate vicinity of the source or in the interstellar medium (ISM) of the host galaxy. Here we discuss different scenarios and possible progenitors for this FRB.

4.1 Scenario 1: origin in a nearby galaxy

In this scenario, we assume that the bulk of the DM comes from the progenitor source and a host galaxy. FRB 160102's observed high DM and RM are indicative of either (i) a rotation-powered scenario in which giant pulses are produced by young energetic pulsars with high spin-down energies (Connor et al. 2016; Cordes & Wasserman 2016) or (ii) a magnetically powered scenario in which radio emission accompanies magnetar hyperflares (Popov & Postnov 2010; Lyubarsky 2014; Lyutikov, Burzawa & Popov 2016).

4.1.1 Pulsars associated with supernova remnants

The influence of supernova remnants (SNRs) on FRBs produced by pulsars within them has been discussed in Connor et al. (2016), Lyutikov et al. (2016), and Piro (2016). In this model, the energy released during an SN explosion by ejecting some amount of mass M_{ej} outward with some velocity v_{ej} is

$$E_{SN} = \frac{1}{2} M_{ej} v_{ej}^2, \qquad (5)$$

where M_{ej} is typically $1.4\,M_\odot$ for a Type Ia SNe and ~ 10–$20\,M_\odot$ for a core-collapse SN, and v_{ej} is typically 10^4 and 5000 km s^{-1} for a Type Ia and core-collapse SNe, respectively (Reynolds 2008). The shock radius scales as $R_s = v_{ej}t$. The outward expanding shock is not influenced by the ISM during the initial free expansion phase but heats it to temperatures sufficient to ionize it. These electrons soon recombine due to the high density. However, as expansion continues interstellar gas accumulates behind the blast shock as it propagates into the ISM, creating a reverse shock that propagates back into the ejecta material and reionizes it creating free electrons that can account for the DM of an FRB.
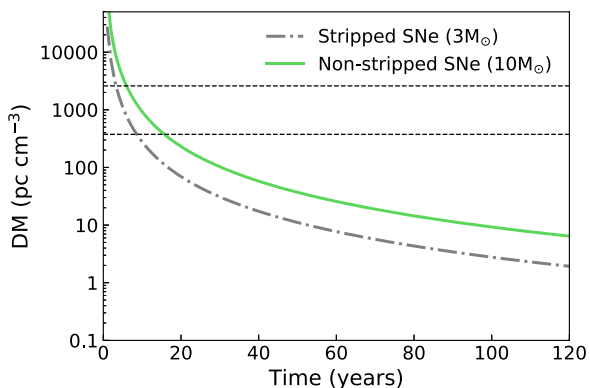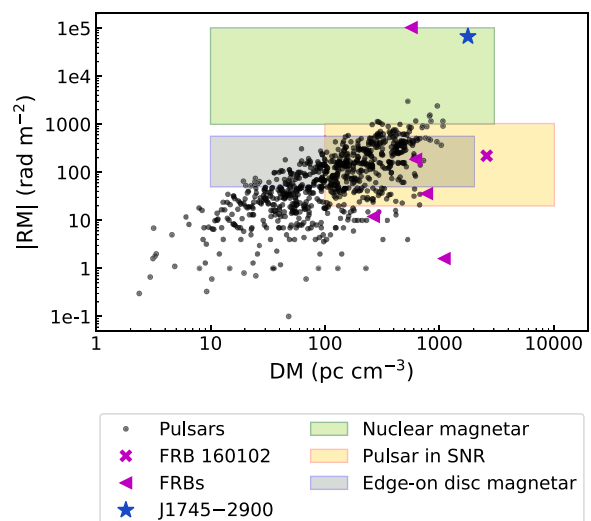
The brightest pulse over the lifetime of the Crab Pulsar would be visible out to $\sim$300 Mpc with current instruments, and similar pulses from other pulsars within this distance could also produce FRBs. If every pulsar within a 100 Mpc distance produces 2×10^5 such pulses over its lifetime, it would be sufficient to reconcile it with the estimated FRB rate (Cordes & Wasserman 2016). For a SNR at 200 Mpc the DM$_{source}$ can be estimated as

$$\begin{aligned} DM_{source} &= DM_{tot} - DM_{host} - DM_{Galaxy} \\ &\quad - DM_{IGM}\ \text{pc cm}^{-3}, \end{aligned} \qquad (6)$$

Table 2. Derived properties of the two FRBs based on the results of RM synthesis. See Section 3.2 for more information.

Event	RM (rad m^{-2})	σ_{RM}	S/N	Polarization amplitude (Jy)	Reduced χ^2
FRB 151230	3355	15	6	0.57	2.4
FRB 160102	−210	13	6	0.48	1.4
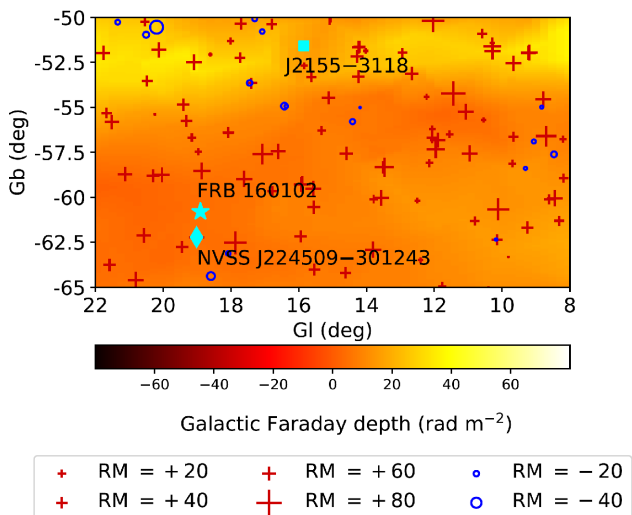
Figure 3. Calibration of the Galactic foreground contribution to the observed RM for FRB 160102. The map represents the Galactic Faraday depth in rad m^{-2} from Oppermann et al. (2015). The negative and positive RMs from the NVSS catalogue (Taylor et al. 2009) are represented by open circles and crosses respectively, with the sizes of the symbols proportional to the RMs. The closest NVSS source and pulsar are represented by the diamond and square, respectively.

Figure 5. Comparison between the RMs and DMs of pulsars and FRBs. The DM values for the FRBs are upper limits as they are the total observed values. The Galactic magnetar J1745−2900 has an unusual LOS that explains the high observed RM. The shaded regions enclose the RM and DM values expected from a pulsar associated with a SNR, a magnetar associated with a galactic centre, and an edge-on disc magnetar. FRB 160102 is seen to be similar to FRB 110523 in RM but with a much higher DM.

Figure 4. DM as a function of age for stripped and non-stripped SNe following Piro (2016). Black dashed lines enclose the range of observed DMs for the known FRBs.

where the redshifting due to frequency is absorbed into the DM$_{source}$ and DM$_{host}$ terms. Bhandari et al. (2018) estimate the contribution from the Milky Way for FRB 160102 to be $\sim$13 pc cm^{-3} and we assume the DM$_{host}$ to be 100 pc cm^{-3} for a median inclination angle of $<70°$ in a Milky Way-type galaxy (Cordes & Lazio 2003; Yao, Manchester & Wang 2017). Based on this we calculate the DM contribution from the SNR to be $\sim$2400 pc cm^{-3} for FRB 160102. Fig. 4 shows the DM as a function of time for stripped (those SNe that have lost most of their initial hydrogen envelope, including most of their helium; 3 M$_\odot$) and non-stripped (10 M$_\odot$)

SNe assuming an ejecta mass M$_{ej}$ = 3 M$_\odot$ expanding with a typical velocity v_{ej} = 10^4 km s^{-1}. A DM of $\sim$2400 pc cm^{-3} is expected at $\sim$3 and $\sim$6 yr after the explosion for stripped and non-stripped SNe, respectively. Piro (2016) shows that free–free absorption in the SNR plays an important role in the propagation of the FRB pulse and can dominate on time-scales of $\sim$100–500 yr. This is backed up observationally by Bietenholz & Bartel (2017). Their very long baseline interferometry (VLBI) and Very Large Array (VLA) observations of the core-collapse SN 1986J reveal a central, bright radio source that helps place constraints on the propagation of a radio pulse through the SN ejecta. They conclude that the SN would have to be a few decades old before it is optically thin enough to a $\sim$1 GHz signal, by which time it would not be possible for the ejecta to produce the observed high DM values seen in FRBs. If the SNR were to produce the observed DM after it becomes optically thin, it would require an unrealistically large portion of the ejecta to be ionized. This implies that for FRB 160102 the majority of the DM is unlikely to originate in the vicinity of the progenitor, suggesting a cosmological origin.

If FRBs are similar to giant pulses from the Crab Pulsar with a similar birth period, and are emitted during the initial 10^3 yr of the progenitor's lifetime, the time interval between repeat pulse is tens to hundreds of hours or longer. However if FRBs are rare and occur randomly during the source's lifetime (e.g. $\gtrsim$1 Gyr), repeat pulses are seen over tens to hundreds of years or longer (Cordes & Wasserman 2016). In such a scenario, it is difficult to place

constraints on the repeat rates and classify an FRB as a one-off event or repeater.

The Galactic large-scale magnetic fields obtained from Faraday rotation measurements of pulsars lie between 1.5 and 2 G in magnitude. Fields can be as high as 11.2 G within the central 4 kpc Galactocentric radius (Haverkorn 2015). More recently, Mao et al. (2017) have determined the existence of coherent G magnetic fields in a galaxy at $z = 0.439$. The average LOS magnetic field towards FRB 160102 without z correction is $B > 0.1$ G that is well below the typical value from our Galaxy. Lyutikov et al. (2016) suggest that this could be due to the fact that the magnetic field giving rise to the RM is confined to the expanding shell. This is supported by Piro (2016), who shows that the RM can be reasonably explained by SNR magnetic fields and that the electrons producing the RM are likely different from the ones producing the DM, as the DM contribution is likely small during the time when the radio pulse can propagate through the SNR environment. Therefore the model of a pulsar associated with a SNR in a nearby galaxy is ruled out for FRB 160102 due to its inability to account for the large observed DM and the absence of an SN within the error region of the FRB position.

4.1.2 Magnetars in galactic centres

The model of magnetars in galactic centres put forth by Pen & Connor (2015) proposes that FRBs are produced by radio-loud magnetars located near the nuclei of galaxies within a few hundred Mpc, i.e. $z \ll 1$. The repeat time-scales for hyperflares or similar events from magnetars are expected to be of the order of hundreds of years, except in the case where the magnetar is young and resides in an intensive star-forming region (Popov & Postnov 2010) in which case the time-scales are shorter, thus providing an explanation for repeating FRBs (Popov, Postnov & Pshirkov 2018). The revelation that FRB 121102 originates in a dwarf galaxy, points to hydrogen-poor superluminous supernovae (SLSNe) and long gamma-ray bursts (LGRBs) as being possible progenitors of the source producing the radio pulses. These classes of transient events have been theorized to produce magnetars with high magnetic fields of $\sim 10^{14}$ G and millisecond spin periods (Metzger, Berger & Margalit 2017; Nicholl et al. 2017). The magnetar at the centre of our Galaxy, J1745−2900, has a measured DM of 1778 ± 3 pc cm^{-3} and RM of $(-6.696 \pm 0.005) \times 10^4$ rad m^{-2} (Eatough et al. 2013). The RM has since changed by 5.3 per cent, to RM $= (-6.340 \pm 0.023) \times 10^4$ rad m^{-2} (Desvignes et al. 2018) with only a marginal DM variation of 1 per cent that is similar to what has been reported for the repeating FRB 121102 (Michilli et al. 2018). Therefore in the case of a circumnuclear source in a nearby galaxy, one might expect RMs of 10^{3-5} rad m^{-2} similar to the magnetar in our Galaxy (Pen & Connor 2015) that is inconsistent with the observed RM of FRB 160102 (see Fig. 5).

Unlike FRBs whose scattering tails are typically ∼milliseconds broad, J1745−2900 is seen to be scattered to ∼second at ∼GHz frequencies. This scattering however is influenced by a screen closer to our Sun than the Galactic Centre, as shown by VLBI measurements (Spitler et al. 2014). This implies that for an extragalactic observer, a typical LOS would only see scattering of the order of milliseconds. Circular polarization is significant in magnetar single pulses (Kramer et al. 2007; Eatough et al. 2013; Shannon & Johnston 2013) and is not uncommon in other radio sources like pulsars. Single pulses from the Crab Pulsar have been seen to be polarized with

a high degree of linear and circular polarization (Słowikowska et al. 2015). This circular polarization is consistent with both FRB 140514 (Petroff et al. 2015) and FRB 160102. Given that J1745−2900 is the only known radio-loud magnetar associated with a nuclear region, it is too soon to extrapolate and interpret the extent to which magnetars form preferentially in galactic centres. However the similarity in RMs between FRB 121102 and J1745−2900, and the significant difference in RMs between FRB 160102 and J1745−2900 is suggestive of two progenitors for these FRBs.

4.2 Scenario 2: origin at cosmological distance

In this scenario, we assume that the bulk of the DM comes from the IGM with only a marginal contribution from the host galaxy and immediate vicinity of the progenitor source.

4.2.1 Binary neutron star mergers

All the models described in the previous sections imply repetitiveness. However, the vast majority of the FRBs have not yet shown repetition despite extensive monitoring in the radio. This could potentially be due to limited sensitivity, insufficient time on sky, the existence of more than one class of FRBs, or a combination of these.

Binary neutron star (BNS) mergers (Totani 2013; Yamasaki, Totani & Kiuchi 2018) are cataclysmic events that justify the non-repeating nature of FRBs. The high end of the range for the BNS merger rate ($\sim 1 \times 10^4$ Gpc^{-3} yr^{-1}; Abadie et al. 2010) is close to the estimated FRB event rate ($\sim 2 \times 10^4$ Gpc^{-3} yr^{-1}; Thornton et al. 2013; Kulkarni et al. 2014). In this model, the FRB is produced by radio emission at the time of the merger due to magnetorotational energy production on a millisecond time-scale. Since polarization is driven by the existence of magnetic fields, any radio emission from BNS mergers can be expected to be polarized. Masui et al. (2015) favour SNRs and highly magnetized, dense star-forming regions for FRBs with high RM values (e.g. FRB 110523), and Yamasaki et al. (2018) favour much cleaner environments implying negligible magnetization in the circumburst plasma, like those expected around BNS mergers for FRBs with small RM values (e.g. FRB 150807). In the case of FRB 160102, a BNS merger at a cosmological distance cannot account for the observed RM. Rather, a fraction of BNS mergers at cosmological distances leaving behind a stable remnant neutron star that may produce faint and repeating FRBs is preferred as this can account for both the observed DM and RM.

4.2.2 Young stellar objects

In this scenario for FRB 160102, we assume a DM of ~ 2480 pc cm^{-3} to arise from the IGM after accounting for a Galactic contribution of ~ 13 pc cm^{-3} and a host galaxy contribution of 100 pc cm^{-3} for a median inclination angle of $< 70°$ in a Milky Way-type galaxy (Cordes & Lazio 2003; Yao et al. 2017). This places FRB 160102 at a redshift of $z \leq 2$ and we calculate the RM at this redshift to be ~ -2400 rad m^{-2} or larger in magnitude (see equation 3). Such values of RM can be produced by models involving young stellar populations like magnetars (Masui et al. 2015; Beloborodov 2017).

Similar to the SN model in Section 4.1.1, magnetars also emit an outflow of magnetized, relativistic winds resulting in a magnetar wind nebula (MWN; Lyubarsky 2014; Murase, Kashiyama &

Mészáros 2016; Beloborodov 2017). An energetic pulse is generated as a result of the disconnection and reconnection of the magnetic field lines that propagates through the magnetar's relativistic wind and creates a relativistic forward shock upon interaction with the plasma. The millisecond duration radiation producing an FRB-like event would be due to coherent synchrotron maser emission from the shock front (Popov & Postnov 2013; Lyubarsky 2014; Beloborodov 2017). The ionized MWN produces the observed linear polarization and RM. This model predicts millisecond, high-energy TeV bursts to accompany the FRB pulse due to the synchrotron radiation at the forward relativistic shock front. However if the flare originates at distances greater than a few to tens of Mpc, it is impossible for current γ-ray monitors to detect these bursts. The giant flare ($\sim 10^{42}$ erg s^{-1}) from the Galactic SGR 1806−20 on 2004 December 27 would only be detectable out to ~ 30−40 Mpc, while the *Swift* telescope can detect similar flares out to ~ 70 Mpc (Hurley et al. 2005). Observations by future observatories like the Cerenkov Telescope Array and Very Energetic Radiation Imaging Telescope Array (VERITAS) are expected to be able to detect bursts from distances ~ 100 Mpc and can prove or falsify this model (Lyubarsky 2014; Murase et al. 2016; Popov et al. 2018).

4.3 Constraints on scattering measure

Temporal broadening is caused by multipath propagation of radiation upon interaction with electron density inhomogeneities and turbulent plasma along the path of propagation thereby altering the observed pulse profile. The angles through which the frequencies are scattered relative to the radiation that travels along the LOS, determine the time delay due to the divergence followed by the convergence back into the LOS. As the strength of the scattering increases so does the angle and time delay and is related to the LOS integral of the plasma–density fluctuation power spectrum and is called the scattering measure (SM). FRBs that exhibit scattering, show temporal broadening consistent with propagation through turbulent plasma (Lorimer et al. 2007; Macquart & Koay 2013; Thornton et al. 2013; Champion et al. 2016). The contribution to the observed SM arises from the plasma fluctuations in the host galaxy of the FRB, the Milky Way, and the IGM. We can rule out the possibility of Galactic contribution to the pulse broadening in the case of FRBs, as high Galactic latitude pulsars exhibit temporal broadening that are orders of magnitude smaller (Bhat et al. 2004; Krishnakumar et al. 2015). According to Macquart & Koay (2013) the scattering expected in the IGM for a given DM is much smaller than that due to the scattering seen in the Milky Way's ISM. Caleb et al. (2016) in their Monte Carlo simulations of a cosmological population of FRBs show that they are unable to fit for the observed widths of the FRBs even after accounting for a scattering model for the IGM. They rule out the possibility of the scattering being LOS dependent following Macquart & Koay (2013), given that the probability of interaction with the ISM of an intervening galaxy or an intracluster medium along the LOS is low. They conclude that the observed widths are likely to be dominated by a component intrinsic to the host galaxy or local environment. This conclusion is backed by Cordes et al. (2016) who suggest that the inability of the IGM to contribute to the temporal scattering of the FRB pulse, implies that ionized regions in host galaxies must be responsible.

The pulse width of FRB 160102 is consistent with a temporally unresolved pulse due to a combination of uncorrected DM smearing in the individual frequency channels and interstellar scattering. Fig. 6 shows a comparison of the SMs for pulsars and two FRBs. A
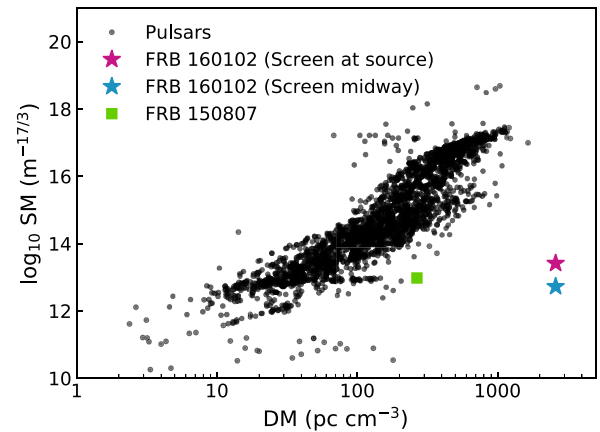

Figure 6. Comparison of scattering measures (SMs) of pulsars and FRB 160102.

standard thin screen model is assumed at the source and mid-way between the source and observer for

$$SM = 2.73 \times 10^{17}(1 + z_{scr})^{17/6}(\nu/1\,\text{GHz})^{11/3}$$
$$\times [\tau_s(D_{eff}/1\,\text{Gpc})^{-1}]^{5/6}\,\text{m}^{-17/3}, \tag{7}$$

where ν is the observing frequency, z_{scr} is the screen redshift, and $D_{eff} = (D_R D_S)/(D_{RS})$, where D_R is the observer–scattering screen distance, D_S is the observer–source distance, and D_{RS} is the source–screen distance. Given $\tau_s = 3.95$ ms at 1 GHz (Bhandari et al. 2018) and assuming the screen to be in the host galaxy ($z \sim 2$ for the total observed DM), we compute the SM to be 3×10^{13} m$^{17/3}$. If the screen is mid-way between the source and observer ($D_{eff} = 2.7$ Gpc; $z \sim 0.77$),we calculate the SM to be 5×10^{12} m$^{17/3}$. From Fig. 6, the value for FRB 160102 appears to be much lower than expected implying less turbulence in the IGM. A large sample of cosmological DMs and SMs would prove invaluable in ascertaining the DM above which transients would be rendered undetectable.

4.4 Effect of scattering on position angle

It is well established from the observations of pulsars that scattering does not only affect the total power of the shape of the total intensity pulse profile, but also its measured polarization properties (e.g. Li & Han 2003; Kramer & Johnston 2008; Karastergiou 2009). While all Stokes parameters are affected, including potentially the inferred degree of polarization, the impact of scattering is easily recognizable from a flattening of the position angle (PA) swing towards later pulse phases (Li & Han 2003), which in the presence of so-called orthogonal polarization modes can also cause an apparent RM variation across the pulse phase (Karastergiou 2009; Noutsos et al. 2015). In the presence of scattering, similar effects should also be expected for FRBs. Because of the shortness of the burst duration, it is difficult to infer a swing of the PA in general, but in cases where PA variations may be seen, scattering would tend to wash out features, which could otherwise provide clues for the underlying origin of the FRBs. Even in cases where scattering is hardly detectable in total power, its impact on the PA may still be important and preventing a correct interpretation of the PA (see Kramer & Johnston 2008; Karastergiou 2009). The PAs for FRB 160102 in Fig. 1 indicate a negative slope with the suggestion of a flattening of the PA at the latest pulse phases. However, the PA uncertainties for the two FRBs are too large and the burst durations are too short to draw any firm conclusions, but we urge consideration of the impact
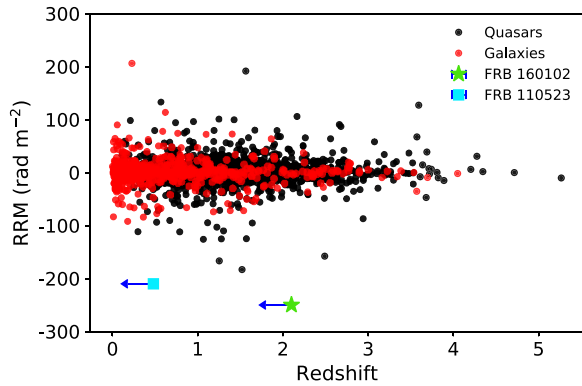
Figure 7. Comparison of the residual rotation measures (RRMs) of galaxies and quasars with FRBs, as a function of redshift. The FRB redshifts are upper limits as they are inferred from their DMs, and would decrease depending on the DM contribution from the host galaxy and environment local to the progenitor. FRB 121102 has been excluded from the plot for clarity.

of scattering when interpreting the polarization properties of FRBs in general.

4.5 Extragalactic rotation measures

Several studies have been used to probe the extragalactic magnetic fields by analysing the residual rotation measures (RRM; the difference between the observed RM and the Galactic RM contribution) as a function of redshift (Reinhardt 1972; Kronberg & Perry 1982; Kronberg et al. 2008). Though these studies report a mean RM of zero out to $z \sim 4$, the evolution of the RRM with redshift due to intervening filaments/clouds and absorbers remains debatable. Simulations by Akahori & Ryu (2011) show that the RMs from the cosmic web would only be a few rad m^{-2}. Pshirkov, Tinyakov & Urban (2016) derived a statistically robust Universe-wide magnetic field strength of $\lesssim 0.65$ nG using the RMs of 3053 high-latitude sources from the NVSS catalogue. Mao et al. (2017) report measurements of coherent G magnetic fields in a lensed galaxy at $z = 0.439$ using broad-band polarization data, similar in strength to galaxies in the local volume.

Hammond, Robishaw & Gaensler (2012) report the largest RRM–redshift catalogue composed of 3650 high-latitude sources. Fig. 7 shows the sources from their RRM–redshift catalogue in comparison with FRB 160102. The FRB RM is inconsistent with the RMs of quasars and galaxies. In case of the FRB, a DM will accompany any RM and there may be multiple gas components that will contribute to both DM and RM with varying proportions. Hence we cannot infer anything concrete from this comparison without an accurate localization.

4.6 Search for repeat pulses

We have monitored fields of FRBs 151230 and 160102 over several months since their discovery to search for repeat pulses. We spent a total of 37.2 h for FRB 151230 and 38.8 h for FRB 160102 with the Parkes Multibeam Receiver centred on the coordinates of the detection beam and detected no pulses with the real-time processing pipeline described in Section 2.1. We searched the data offline for pulses down to S/N > 5 and still detected no pulses. Searches for repeats in these fields are ongoing, and strongly encouraged.

5 SUMMARY AND CONCLUSION

In this paper we present the properties of two FRBs reported in Bhandari et al. (2018). FRBs 151230 and 160102 were found to have linear and circular polarization fractions of $L = 35 \pm 13$ per cent, $V = 6 \pm 11$ per cent at RM = 0 rad m^{-2} and $L = 84 \pm 15$ per cent, $V = 30 \pm 11$ per cent at RM = -220.6 rad m^{-2}, respectively. The average Galactic foreground contribution for the latter was estimated to be $+28 \pm 6$ rad m^{-2} implying RM$_{source}$ + RM$_{host}$ = -256 ± 9 rad m^{-2} ignoring the correction due to redshifting of frequency and assuming RM$_{IGM}$ = $+7$ rad m^{-2}.

Based on the observed RM we discuss possible progenitor scenarios for FRB 160102. In the case of a pulsar associated with an SNR (see Section 4.1.1), after accounting for the Galactic and a possible host contribution to the DM, the implied source DM of ~ 2400 pc cm^{-3} is expected ~ 3 and ~ 6 yr after the explosion for stripped and non-stripped SNe, respectively. The expected dominance of free–free absorption during these years would hinder the propagation of a radio wave. Therefore, the SNe would have to be at least a few decades old before it is optically thin to a ~ 1 GHz signal by which time the ejecta would be too diffuse to contribute much to the large observed DM.

The large DM and RM of this FRB along with the observed linear and circular fractional polarizations can be explained by the model proposing that FRBs are from magnetars associated with galactic centres (see Section 4.1.2). On the other hand, the very rare occurrence of known magnetars close to a galactic nucleus prevents any meaningful quantification of the likelihood of this hypothesis.

We also consider explosion-based events such as BNS mergers at cosmological distances. While the BNS merger itself cannot quite explain the high RM value, a stable neutron star remnant of the merger could potentially provide the observed high RM but would also imply repeatability (see Section 4.2.1). Again, in the cosmological scenario, assuming the majority of the DM to arise from the IGM, we place FRB 160102 at $z \leq 2$. The RM at source for this redshift is ~ -2400 rad m^{-2} or larger in magnitude that is indicative of stellar models involving a young population such as magnetars (see Section 4.2.2).

The SM for FRB 160102 based on the observed scattering at 1 GHz is seen to be much lower than what is expected thereby implying less turbulence in the IGM than usually assumed. We also observed a flattening of the polarization position angle swing for this FRB. However, a firm interpretation of that as due to the effect of scattering is hampered by the short duration of the burst and the uncertainty in measurement of the polarization PA. We have compared the RM with the published extragalactic RMs of quasars and galaxies, but no secure association of FRB 160102 with a kind of known radio source could be established. It should be noted that multiple gas components along the LOS will alter the DM and RM. Thus no strong conclusions can be arrived at without accurate localization of the FRB.

REFERENCES

Abadie J. et al., 2010, Classical Quantum Gravity, 27, 173001
Akahori T., Ryu D., 2011, ApJ, 738, 134
Akahori T., Ryu D., Gaensler B. M., 2016, ApJ, 824, 105
Bannister K. W., Madsen G. J., 2014, MNRAS, 440, 353
Beloborodov A. M., 2017, ApJ, 843, L26
Bhandari S. et al., 2018, MNRAS, 475, 1427
Bhat N. D. R., Cordes J. M., Camilo F., Nice D. J., Lorimer D. R., 2004, ApJ, 605, 759
Bietenholz M. F., Bartel N., 2017, ApJ, 851, 124
Bower G. C., Wright M. C. H., Falcke H., Backer D. C., 2003, ApJ, 588, 331
Brentjens M. A., de Bruyn A. G., 2005, A&A, 441, 1217
Caleb M., Flynn C., Bailes M., Barr E. D., Hunstead R. W., Keane E. F., Ravi V., van Straten W., 2016, MNRAS, 458, 708
Champion D. J. et al., 2016, MNRAS, 460, L30
Connor L., Sievers J., Pen U.-L., 2016, MNRAS, 458, L19
Cordes J. M., Lazio T. J. W., 2003, preprint (arXiv:0207156)
Cordes J. M., Wasserman I., 2016, MNRAS, 457, 232
Cordes J. M., Wharton R. S., Spitler L. G., Chatterjee S., Wasserman I., 2016, preprint (arXiv:1605.05890)
Desvignes G. et al., 2018, ApJ, 852, L12
Eatough R. P. et al., 2013, Nature, 501, 391
Falcke H., Rezzolla L., 2014, A&A, 562, A137
Fuller J., Ott C. D., 2015, MNRAS, 450, L71
Hammond A. M., Robishaw T., Gaensler B. M., 2012, preprint (arXiv:1209.1438)
Han J. L., Manchester R. N., Lyne A. G., Qiao G. J., van Straten W., 2006, ApJ, 642, 868
Han J. L., Manchester R. N., van Straten W., Demorest P., 2018, ApJS, 234, 11
Haverkorn M., 2015, in Lazarian A., de Gouveia Dal Pino E. M., Melioli C., eds, Astrophysics and Space Science Library Vol. 407, Magnetic Fields in Diffuse Media. Springer-Verlag, Berlin, p. 483
Hotan A. W., Bailes M., Ord S. M., 2005, MNRAS, 362, 1267
Hurley K. et al., 2005, Nature, 434, 1098
Johnston S., 2004, MNRAS, 348, 1229
Karastergiou A., 2009, MNRAS, 392, L60
Kashiyama K., Ioka K., Mesaros P., 2013, ApJ, 776, L39
Keane E. F. et al., 2016, Nature, 530, 453
Keane E. F. et al., 2018, MNRAS, 473, 116
Kramer M., Johnston S., 2008, MNRAS, 390, 87
Kramer M., Stappers B. W., Jessner A., Lyne A. G., Jordan C. A., 2007, MNRAS, 377, 107
Krishnakumar M. A., Mitra D., Naidu A., Joshi B. C., Manoharan P. K., 2015, ApJ, 804, 23
Kronberg P. P., 2016, Cosmic Magnetic Fields. Cambridge Univ. Press, Cambridge
Kronberg P. P., Perry J. J., 1982, ApJ, 263, 518
Kronberg P. P., Bernet M. L., Miniati F., Lilly S. J., Short M. B., Higdon D. M., 2008, ApJ, 676, 70

Kulkarni S. R., Ofek E. O., Neill J. D., Zheng Z., Juric M., 2014, ApJ, 797, 70
Li X. H., Han J. L., 2003, A&A, 410, 253
Lorimer D. R., Bailes M., McLaughlin M. A., Narkevic D. J., Crawford F., 2007, Science, 318, 777
Lyubarsky Y., 2014, MNRAS, 442, L9
Lyutikov M., Burzawa L., Popov S. B., 2016, MNRAS, 462, 941
Macquart J.-P., Koay J. Y., 2013, ApJ, 776, 125
Macquart J.-P., Ekers R. D., Feain I., Johnston-Hollitt M., 2012, ApJ, 750, 139
McQuinn M., 2014, ApJ, 780, L33
Mao S. A. et al., 2017, Nat. Astron., 1, 621
Marrone D. P., Moran J. M., Zhao J.-H., Rao R., 2007, ApJ, 654, L57
Masui K. et al., 2015, Nature, 528, 523
Metzger B. D., Berger E., Margalit B., 2017, ApJ, 841, 14
Michilli D. et al., 2018, Nature, 553, 182
Murase K., Kashiyama K., Mészáros P., 2016, MNRAS, 461, 1498
Nicholl M., Williams P. K. G., Berger E., Villar V. A., Alexander K. D., Eftekhari T., Metzger B. D., 2017, ApJ, 843, 84
Noutsos A., Johnston S., Kramer M., Karastergiou A., 2008, MNRAS, 386, 1881
Noutsos A. et al., 2015, A&A, 576, A62
Oppermann N. et al., 2015, A&A, 575, A118
Pen U.-L., Connor L., 2015, ApJ, 807, 179
Petroff E., Bailes M., Barr E. D., Barsdell B. R., Bhat N. D. R., Bian F., Burke-Spolaor S., Caleb M., 2015, MNRAS, 447, 246
Petroff E. et al., 2016, Publ. Astron. Soc. Aust., 33, e045
Petroff E. et al., 2017, MNRAS, 469, 4465
Piro A. L., 2016, ApJ, 824, L32
Popov S. B., Postnov K. A., 2010, in Harutyunian H. A., Mickaelian A. M., Terzian Y., eds, Evolution of Cosmic Objects through Their Physical Activity. 'Gitutyun' Publishing House, National Academy of Sciences of the Republic of Armenia (NAS RA), p. 129
Popov S. B., Postnov K. A., 2013, preprint (arXiv:1307.4924)
Popov S. B., Postnov K. A., Pshirkov M. S., 2018, preprint (arXiv:1801.00640)
Pshirkov M. S., Tinyakov P. G., Urban F. R., 2016, Phys. Rev. Lett., 116, 191302
Ravi V. et al., 2016, Science, 354, 1249
Reinhardt M., 1972, A&A, 19, 104
Reynolds S. P., 2008, ARA&A, 46, 89
Schnitzeler D. H. F. M., 2010, MNRAS, 409, L99
Schnitzeler D. H. F. M., Lee K. J., 2015, MNRAS, 447, L26
Shannon R. M., Johnston S., 2013, MNRAS, 435, L29
Słowikowska A., Stappers B. W., Harding A. K., O'Dell S. L., Elsner R. F., van der Horst A. J., Weisskopf M. C., 2015, ApJ, 799, 70
Sotomayor-Beltran C. et al., 2013, A&A, 552, A58
Spitler L. G. et al., 2014, ApJ, 780, L3
Staveley-Smith L. et al., 1996, Publ. Astron. Soc. Aust., 13, 243
Taylor A. R., Stil J. M., Sunstrum C., 2009, ApJ, 702, 1230
Thornton D. et al., 2013, Science, 341, 53
Totani T., 2013, PASJ, 65, L12
van Straten W., 2013, ApJS, 204, 13
van Straten W., Manchester R. N., Johnston S., Reynolds J. E., 2010, Publ. Astron. Soc. Aust., 27, 104
Yamasaki S., Totani T., Kiuchi K., 2018, PASJ, in press (arXiv:1710.02302)
Yao J. M., Manchester R. N., Wang N., 2017, ApJ, 835, 29
Zheng Z., Ofek E. O., Kulkarni S. R., Neill J. D., Juric M., 2014, ApJ, 797, 71
Zhou B., Li X., Wang T., Fan Y.-Z., Wei D.-M., 2014, Phys. Rev. D, 89, 107303

This paper has been typeset from a TEX/LATEX file prepared by the author.